AD_____

Award Number: DAMD17-98-1-8164

TITLE: Tumor Targeting Peptides for Cytotoxic Chemotherapy Delivery

PRINCIPAL INVESTIGATOR: Kimmo Porkka, M.D., Ph.D.

CONTRACTING ORGANIZATION: The Burnham Institute
La Jolla, California 92307

REPORT DATE: July 2001

TYPE OF REPORT: Annual Summary

PREPARED FOR: U.S. Army Medical Research and Materiel Command
Fort Detrick, Maryland 21702-5012

REPORT DOCUMENTATION PAGE

Form Approved
OMB No. 074-0188

1. AGENCY USE ONLY (Leave blank)	2. REPORT DATE	3. REPORT TYPE AND DATES COVERED
	July 2001	Annual Summary (1 Jul 98 - 30 Jun 01)

4. TITLE AND SUBTITLE
Tumor Targeting Peptides for Cytotoxic Chemotherapy Delivery

5. FUNDING NUMBERS
DAMD17-98-1-8164

6. AUTHOR(S)
Kimmo Porkka, M.D., Ph.D.

7. PERFORMING ORGANIZATION NAME(S) AND ADDRESS(ES)
The Burnham Institute
La Jolla, California 92307

E-Mail: ruoslahti@burnham.org

8. PERFORMING ORGANIZATION REPORT NUMBER

9. SPONSORING / MONITORING AGENCY NAME(S) AND ADDRESS(ES)
U.S. Army Medical Research and Materiel Command
Fort Detrick, Maryland 21702-5012

10. SPONSORING / MONITORING AGENCY REPORT NUMBER

11. SUPPLEMENTARY NOTES
Original contains color plates: All DTIC reproductions will be in black and white.

12a. DISTRIBUTION / AVAILABILITY STATEMENT
Approved for Public Release; Distribution Unlimited.

12b. DISTRIBUTION CODE

13. ABSTRACT ***(Maximum 200 Words)***

Tumors cannot grow without a blood supply. The distinct characteristics of tumor vasculature make it possible to design therapeutic agents that specifically target the tumor, but not normal blood vessels. Identifying tools for therapeutic tumor targeting was the focus of the project. A new tumor-homing phage (F3) was isolated by combining *ex vivo* screening of a phage cDNA library on cell suspensions prepared from bone marrow and *in vivo* screening for tumor homing. The F3 phage recognizes the blood vessels in the MDA-MB-435 breast cancers and HL-60 leukemia xenograft tumors. Fluorescein-labeled F3, injected intravenously into mice, accumulates in the endothelium of tumor blood vessels. Small subpopulations of cells in the skin, gut, and bone marrow also pick up F3, but the vessels in normal tissues are all negative. F3 may be a marker of certain progenitor cells. Importantly, the F3 peptide can carry a payload, such as the fluorescein label, into the nucleus of the target cells. It may be particularly well suited as a carrier of drugs that act in the nucleus.

14. SUBJECT TERMS	15. NUMBER OF PAGES
Angiogenesis, tumor vasculature, peptides, drug targeting, progenitor cells	18
	16. PRICE CODE

17. SECURITY CLASSIFICATION OF REPORT	18. SECURITY CLASSIFICATION OF THIS PAGE	19. SECURITY CLASSIFICATION OF ABSTRACT	20. LIMITATION OF ABSTRACT
Unclassified	Unclassified	Unclassified	Unlimited

DAMD17-98-1-8164
Tumor Targeting Peptides for Cytotoxic Chemotherapy Delivery
PI: Kimmo Porkka, M.D., Ph.D.

INTRODUCTION

Tumors cannot grow without a blood supply. To secure a blood supply, they take over existing blood vessels and promote angiogenesis—the sprouting of new vessels from existing ones. Initiation of angiogenesis (the angiogenic switch) is an important early event in tumour progression, and neovascularization begins in pre-malignant lesions. Because tumor vessels are growing and because they reside in a tumor environment, these vessels are distinct from normal resting blood vessels. The distinct characteristics of tumor vasculature make possible to design therapeutic agents that specifically target the vessels in the tumor, but not normal blood vessels. Tumor blood vessels make excellent therapeutic targets because they are available to agents in the blood stream and because they do not possess the genetic instability that allows cancer cells to develop drug resistance. Identifying tools for therapeutic targeting was the focus of this project, for which this final report is written.

Dr. Erkki Ruoslahti's laboratory, where the work was done, uses libraries of phage-displayed peptides to identify specific changes in tumor vasculature, particularly the vasculature of breast cancers. I have used a modification of this procedure to identify a novel peptide that homes to MDA-MB-435 breast cancer and other xenografts grown in mice.

DESCRIPTION OF THE TRAINING

Kimmo Porkka, MD, PhD. received research training in clinical epidemiology, clinical cancer research, and human molecular genetics. His clinical training includes specialist degrees in internal medicine and clinical hematology. To complement his clinical training, he worked in Dr. Erkki Ruoslahti's laboratory at The Burnham Institute in La Jolla from April 1999 to June 2001, after which he returned to the Department of Hematology at the University of Helsinki. He also has a laboratory and an adjunct appointment at Biomedicum Helsinki, a basic research unit at the University. The stay at The Burnham Institute allowed Dr. Porkka to become proficient in molecular biology and vascular biology research. His current position as a physician scientist in Helsinki attests to the effectiveness of the experience he gained during his stay in La Jolla.

RESULTS

A new tumor-homing phage (F3) was isolated by combining *ex vivo* screening of a phage cDNA library on cell suspensions prepared from bone marrow and *in vivo* screening for tumor homing. The F3 phage recognizes the blood vessels in the MDA-MB-435 breast cancer and HL-60 leukemia xenograft tumors. The F3 cDNA in the phage encodes a 31-amino acid fragment of a nuclear protein, HMGN2. Whether the apparent affinity of the fragment for cell surfaces somehow reflects a physiological binding function of HMGN2, is not known.

We prepared the HMGN2 fragment as a labeled synthetic peptide and studied its distribution in tissues and cell cultures. Intravenously injected synthetic F3 peptide also homes to tumor vasculature. Fluorescein-labeled F3 is detected in the endothelium of tumor blood vessels, but not other blood vessels. The tumor cells also pick up fluorescein-F3, as do small subpopulations of cells in the skin and gut. However, unlike the tumor blood vessels, the vessels in the skin and gut are negative. Flow cytometry reveals another F3-positive minor population of cells in the bone marrow. We hypothesize, based on these results, that F3 may be a marker of certain progenitor cells. These cells could include endothelial cell progenitors that reside in the bone marrow and are mobilized to participate in angiogenesis. Various tumor cells, such as MDA-MB-435 and HL-60 cells, also appear to have acquired this putative progenitor cell marker.

A remarkable property of the F3 peptide is that it can carry a payload, such as the fluorescein label, all the way to the nucleus of the target cells. This is likely to be due to the high number of basic residues in the sequence of this peptide, which may create a nuclear translocation signal and should also endow the peptide with an ability to bind DNA. The specificity of F3 for tumor vasculature may allow specific targeting of therapies to breast cancers. The translocation of the peptide (and its payload) into the nucleus of tumor endothelial cells and tumor cells may make F3 particularly well suited as a carrier of drugs that act in the nucleus. These results have been reported in a paper that appeared in *PNAS* (Porkka et al., 2002), and drug targeting with F3 is underway in the Ruoslahti laboratory. They have already shown that quantum dots, which are luminescent nanocrystals, can be specifically targeted to MDA-MB-435 tumor vessels by coating the quantum dots with the F3 peptide (Akerman et al., 2002).

I also participated in a project where it was shown that lymphatic vessels in MDA-MB-435 tumors express a specific marker (Laakkonen et al., 2002). The presence and importance of blood vessels in tumors is well established, but it has only recently been found that lymphatic vessels can also be present within tumors. These vessels were previously thought to occur in the normal tissue surrounding tumors. A phage that displays the peptide CGNKRTRGC (Lyp-1) homes to the MDA-MB-435 tumors, when injected either into the bloodstream or subcutaneously. The phage and fluorescein-labeled LyP-1 peptide accumulate in vessel-like structures in the tumors that stain for lymphatic vessel, but not for blood vessel markers. The phage and the peptide do not accumulate in normal tissues, indicating that the LyP-1 peptide distinguishes lymphatic vessels in MDA-MB-435 xenografts from normal lymphatic vessels. Targeting drugs to lymphatic vessels in tumors with this peptide may be particularly effective in preventing tumor metastasis.

KEY RESEARCH ACCOMPLISHMENTS

- Identification of a tumor-homing peptide with a novel specificity for the vasculature of breast cancer and leukemia xenografts.
- Demonstration of nuclear targeting properties of the novel tumor-homing peptide.
- Participation in work demonstrating for the first time that breast cancer lymphatics express a tumor specific marker.

REPORTABLE OUTCOMES

Publications:

1. Porkka, K., Laakkonen, P., Hoffman, J.A., Bernasconi, M. and Erkki Ruoslahti, E. Targeting of peptides to the nuclei of tumor cells and tumor endothelial cells *in vivo*. *PNAS* **99**, 7444-7449, 2002.
2. Laakkonen, P., Porkka, K., Hoffman, J.A. and Erkki Ruoslahti, E. Specialization of tumor lymphatics. *Nature Med.* **8**, 751-755, 2002.

PATENT APPLICATIONS:

P-LJ 5234 IDS, "HMGN Peptides and Related Molecules That Selectively Home To Tumor Blood Vessels and Tumor Cells"

P-LJ 4638, "Methods of Targeting Angiogenic Vasculature Using Gelatinase Inhibitors."

REFERENCES

Akerman, M.A., Chan, W. C. W., Laakkonen, P., Bhatia S.N. and Ruoslahti, E. In vivo targeting of nanocrystals. *PNAS* **99**, 12617-12621, 2002.

Laakkonen, P., Porkka, K., Hoffman, J.A. and Erkki Ruoslahti, E. Specialization of tumor lymphatics. *Nature Med.* **8**, 751-755, 2002.

Porkka, K., Laakkonen, P., Hoffman, J.A., Bernasconi, M. and Erkki Ruoslahti, E. Targeting of peptides to the nuclei of tumor cells and tumor endothelial cells *in vivo*. *PNAS* **99**, 7444-7449, 2002.

A tumor-homing peptide with a targeting specificity related to lymphatic vessels

PIRJO LAAKKONEN[1], KIMMO PORKKA[1], JASON A. HOFFMAN[2] & ERKKI RUOSLAHTI[1]

[1]*Cancer Research Center, The Burnham Institute, La Jolla, California, USA*
[2]*Program in Molecular Pathology, The Burnham Institute and Department of Pathology, University of California San Diego School of Medicine, La Jolla, California, USA*
Correspondence should be addressed to E.R.; email: ruoslahti@burnham.org

Published online: 10 June 2002, doi:10.1038/nm720

Blood vessels of tumors carry specific markers that are usually angiogenesis-related[1,2]. We previously used phage-displayed peptide libraries *in vivo* to identify peptides that home to tumors through the circulation and that specifically bind to the endothelia of tumor blood vessels[3,4]. Here we devised a phage screening procedure that would favor tumor-homing to targets that are accessible to circulating phage, but are not blood vessels. Screening on MDA-MB-435 breast carcinoma xenografts yielded multiple copies of a phage that displays a cyclic 9-amino-acid peptide, LyP-1. Homing and binding to tumor-derived cell suspensions indicated that LyP-1 also recognizes an osteosarcoma xenograft, and spontaneous prostate and breast cancers in transgenic mice, but not two other tumor xenografts. Fluorescein-labeled LyP-1 peptide was detected in tumor structures that were positive for three lymphatic endothelial markers and negative for three blood vessel markers. LyP-1 accumulated in the nuclei of the putative lymphatic cells, and in the nuclei of tumor cells. These results suggest that tumor lymphatics carry specific markers and that it may be possible to specifically target therapies into tumor lymphatics.

We combined *ex vivo* and *in vivo* phage selections[5] to search for peptides that recognize tumor-specific vessels other than blood vessels. We selected phage from a cyclic peptide library for binding to cell suspensions prepared from MDA-MB-435 breast cancer xenografts. To increase the likelihood of obtaining new kinds of homing peptides, we reduced the number of blood vessel endothelial cells by treating the cell suspension with anti-CD31 magnetic beads before recovering and amplifying bound phage. Blood-vessel endothelial cells express high levels of CD31, whereas lower levels are expressed by lymphatic endothelial cells[6,7] (and this study). Three rounds of *ex vivo* selection yielded a phage pool that bound to the primary tumor-derived cells approximately 350-fold over control, non-recombinant phage. Subsequent *in vivo* selections of this pool in a nude mouse bearing an MDA-MB-435 tumor resulted in 30-fold enrichment in the tumor relative to non-recombinant phage.

One of the peptide sequences enriched in the selected phage pool was CGNKRTRGC. The phage displaying this peptide bound to primary MDA-MB-435 tumor-derived cell suspensions about 7,000 times more than non-recombinant phage (Fig. 1*a*). The synthetic CGNKRTRGC peptide (LyP-1) inhibited the binding of the phage (data not shown). The LyP-1 phage bound cultured MDA-MB-435 cells on average about 100-fold over non-recombinant phage. The LyP-1-displaying phage also bound to cell suspensions prepared from KRIB osteosarcoma xenografts, and from transgenic mouse mammary carcinomas (Fig. 1*a*). This phage did not to bind to cell suspensions from HL-60 leukemia or C8161 melanoma xenografts (Fig. 1*a*). Two permutations (CGEKRTRGC and CGNKRTRGV) arose spontaneously during the phage amplification and were recognized because of an altered plaque size. They did not significantly bind to MDA-MB-435 tumor-derived cell suspensions.

The LyP-1-displaying phage homed to the MDA-MB-435 and KRIB tumors *in vivo*. On the average, the mean phage titer in tumor tissue was 60-fold greater than non-recombinant phage in MDA-MB-435 tumors and 15-fold in KRIB tumors (Fig. 1*b*). In agreement with the cell-binding data, the phage did not home *in vivo* to HL-60 or C8161 xenografts (Fig. 1*b*), nor to brain, spleen, skin, kidneys and lungs; there may have been some homing to normal breast tissue (Fig. 1*c*). The MDA-MB-435 homing of the variant CGEKRTRGC-displaying phage was only 10% of the homing of the LyP-1.

When we treated MDA-MB-435 tumor-derived cells with 0.5% NP-40 before recovering homed phage, we found 10–20 times more LyP-1 phage than without the detergent, suggesting that the phage was internalized by cells. *In vitro* experiments showed that cultured MDA-MB-435 cells internalized fluorescein-conjugated LyP-1 peptide. The labeled peptide initially appeared in the cytoplasm and, with time, increasingly in the nucleus (Fig. 1*d*). There was no detectable cellular uptake of a fluorescein-labeled control peptide (ARALPSQRSR), which like CGNKRTRGC has three basic residues (data not shown).

Intravenously (i.v.) injected LyP-1 phage localized to vessel-like structures and to some single cells within the MDA-MB-435 tumors. The vessels containing the phage were negative for CD31 (Fig. 2*a*). Fluorescein-conjugated synthetic LyP-1 peptide, when injected into the tail vein of MDA-MB-435 tumor-bearing mice, also localized to vessel-like structures and to individual cells within the tumor mass. The peptide-stained vessels did not appear to be blood vessels, because they were negative for MECA-32 staining (Fig. 2*b*). In addition, there was a lack of colocalization with blood vessels labeled by i.v.-injected tomato lectin[8]. When the peptide and lectin fluorescence were captured in the same microscopic field, they were separate (Fig. 2*c*), and many fields contained only peptide fluorescence (Fig. 2*d*) or only lectin fluorescence (Fig. 2*e*). Fluorescein-conjugated LyP-1 localized to MDA-MB-435 tumors regardless of whether the tumors were grown subcutaneously or in the mammary fat pad,

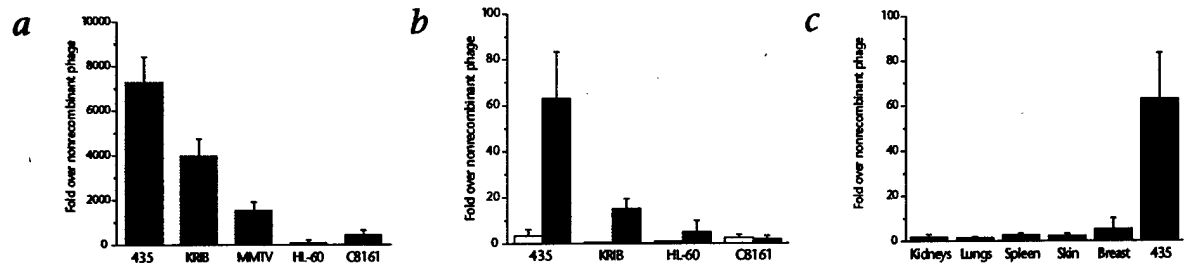

Fig. 1 Tumor homing and binding of LyP-1 phage, and nuclear translocation of synthetic LyP-1 peptide. ***a***, Binding of LyP-1 phage to primary cell suspensions from MDA-MB-435, KRIB xenografts and transgenic mouse mammary carcinomas (MMTV), but not to cells from HL-60 leukemia or C8161 melanoma xenografts. ***b***, *In vivo* homing of the phage. Tumor homing of LyP-1 phage to MDA-MB-435, KRIB, HL-60 and C8161 xenografts after i.v. injection. □, brain; ■, tumor. ***c***, LyP-1 phage titers recovered from kidney, lung, spleen and skin after injection into the tail vein of tumor-bearing mice or from breast tissue after injection into the tail vein of nude mice. ***d***, Internalization of fluorescein-conjugated LyP-1 peptide (green) by cultured MDA-MB-435 cells. Nuclei are visualized by DAPI staining (blue). Error bars represent mean ± s.e.m. for 3–8 experiments per variable.

but more fluorescence accumulated in the subcutaneous tumors (data not shown). The fluorescein-conjugated peptide also homed to transgenic prostate carcinomas (TRAMP), again failing to colocalize with tomato lectin (Fig. 2*f*). Among several normal tissues studied, fluorescence was only seen in kidney tubuli, presumably as a result of uptake of free fluorescein-conjugated LyP-1 from the glomerular filtrate. Fluorescence from the labeled control peptide also localized in kidney tubuli (data not shown).

Our data suggested that the vessel-like structures targeted by LyP-1 were not blood vessels, so we hypothesized that they might be lymphatic vessels. To investigate whether LyP-1 homed to tumor lymphatics, we stained MDA-MB-435 tumor sections with lymphatic markers: lymphatic vessel endothelial hyaloronic acid receptor-1 (LYVE-1), a transmembrane hyaluronic acid receptor[9,10]; podoplanin, a glomerular podocyte membrane protein[11]; and vascular endothelial growth factor receptor-3 (VEGFR-3)[12–14]. In accordance with earlier results[13–15], antibodies against each of these markers stained vessel-like structures in the MDA-MB-435 tumors. These structures frequently lacked a detectable lumen. The staining rarely overlapped with lectin staining, indicating that few, if any, of these vessels were blood vessels.

Fluorescein-conjugated LyP-1 injected into the tail vein of tumor-bearing mice colocalized with LYVE-1 (Fig. 3*a*), podoplanin (Fig. 3*b* and *c*) and VEGFR-3 (Fig. 3*d* and *e*) in vessel-like structures within MDA-MB-435 tumor tissue. Some of these structures appeared to be vessels filled with tumor cells (Fig. 3*f*). LyP-1 also accumulated outside the structures positive for the lymphatic markers, including the tumor cells, individual VEGFR3-positive cells and what appeared to be connective tissue between tumor cells. However, LyP-1 fluorescence typically centered around the structures detected with the lymphatic marker antibodies, implicating the lymphatic structures as the likely primary site of LyP-1 recognition. High-magnification images (Fig. 3*c* and *g*) show that fluorescein-conjugated LyP-1 accumulated in the nuclei of cells lining vessel-like structures, while the lymphatic marker antibodies (anti-podoplanin in Fig. 3*c*) stained the plasma membranes of the same cells. We also injected i.v. mice with monoclonal antibody to podoplanin, and could detect the antibody in tissues. The injected antibody colocalized with LYVE-1 (Supplementary Fig. A online), and LyP-1 (Fig. 3*h*), but not with MECA-32 (data not shown).

The LyP-1 phage did not recognize C8161 xenografts in homing or cell-binding assays, but these tumors did contain vessel-like structures that stained positive for both LYVE-1 and podoplanin, but not for the tomato lectin (Supplementary Fig. B online). These results indicate that LyP-1 recognizes lymphatic vessel-associated structures in some tumors but not in others.

Previous *in vivo* phage-screening experiments have yielded peptides that recognize markers that are selectively expressed in tumor vasculature[3,4]. The structures recognized by LyP-1 in the target tumors seem to be related to lymphatic vessels, rather than blood vessels, as shown by colocalization of LyP-1 with three lymphatic markers and lack of colocalization with three blood-vessel markers. Probes for lymphatic vessels that require transport of the probe through the lymphatic vessels have generally revealed such vessels around, but not within tumors[16–18]. However, the use of molecular markers for lymphatic endothelial cells has revealed lymphatic structures inside many tumors[9,13–15].

Each of the lymphatic markers that we used colocalized with LyP-1 in the MDA-MB-435 tumors. None of these markers are completely specific for lymphatic endothelial cells[19,20], but the presence of all three markers in the LyP-1-positive structures strongly suggests that these structures are lymphatic vessels. These LyP-1-binding cells are not tumor cells, because they stained with antibody against mouse VEGFR-3 and with antibodies against mouse major histocompatibility complex (MHC) antigen H-2K^d (data not shown). The VEGFR-3 antibody is known not to recognize human VEGFR-3 (K. Alitalo and H. Kubo, pers. comm.).

LyP-1 often colocalized with lymphatic markers in structures that appeared in tissue sections as thin strands that form loops. These structures may be collapsed lymphatic vessels. Moreover, the reticular architecture with numerous ill-defined lumina described for tumor lymphatics in the recent study of human head and neck cancers is similar to ours[15]. Alternatively, these struc-

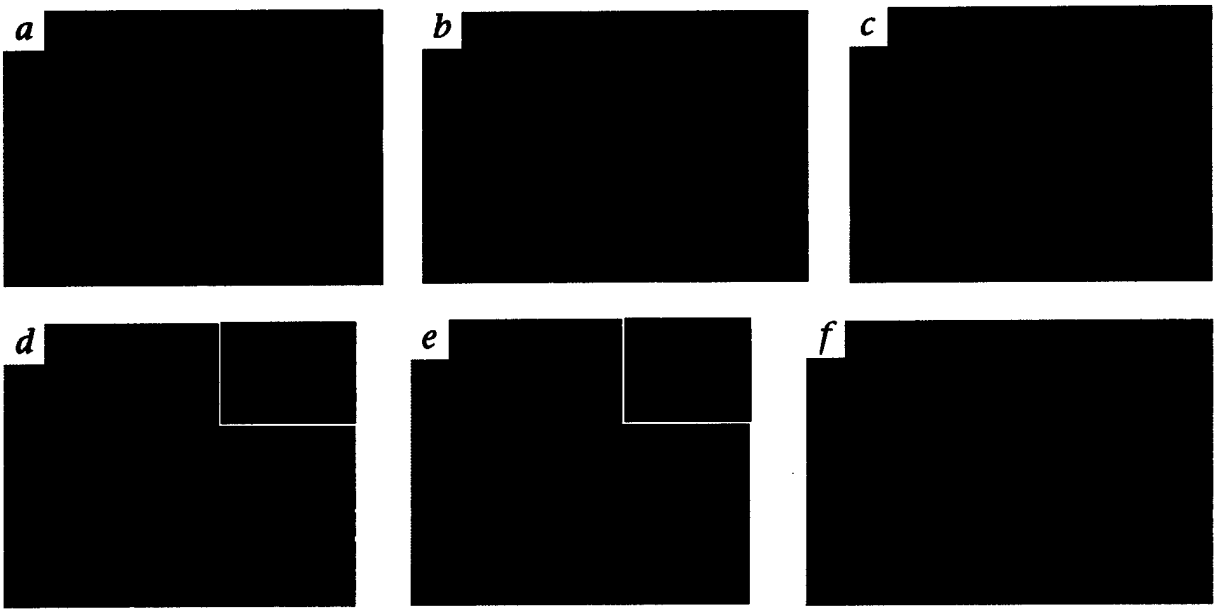

Fig. 2 LyP-1 phage and LyP-1 peptide do not colocalize with blood vessel markers. *a–e*, LyP-1 phage (*a*) or fluorescein-conjugated LyP-1 peptide (*b–e*) injected into the tail vein of a mouse bearing an MDA-MB-435 tumor. *a*, Tumor blood vessels were stained with anti-CD31 antibody (red) and phage was visualized using anti-T7 antibody followed by fluorescein-conjugated anti-rabbit IgG (green). *b–e*, Tumor blood vessels (red) were detected with MECA-32 (*b*) or i.v. injected, biotinylated tomato lectin (*c–e*). The green color shows the localization of LyP-1 peptide. *c*, A microscopic field containing both LyP-1 peptide and lectin fluorescence. *d*, Areas where peptide staining was abundant were often devoid of blood vessels. (the *inset*, blood vessel staining in the same microscopic field) *e*, Other areas of the tumor contained numerous blood vessels, but no peptide (inset, peptide staining in the same microscopic field). *f*, LyP-1 peptide (green) homed also to the transgenic mouse prostate tumor (TRAMP). Blood vessels (red) were detected with i.v. injected biotinylated tomato lectin. *d*, *e* and the insets in *d* and *e* are single color images. Magnification, ×400 in *a*, *c*, and *e*; ×200 in *b*, *d* and *f*.

tures could be dilated lymphatic vessels filled with tumor. It may be that most intra-tumor lymphatics are not patent vessels functional in transporting lymph. Because we access the tumor lymphatics through blood circulation, the accumulation of our phage and peptide in these structures may not be dependent on functionality of the targeted lymphatics.

Although these results strongly suggest that LyP-1 binds to tumor lymphatics, we cannot exclude the possibility that the

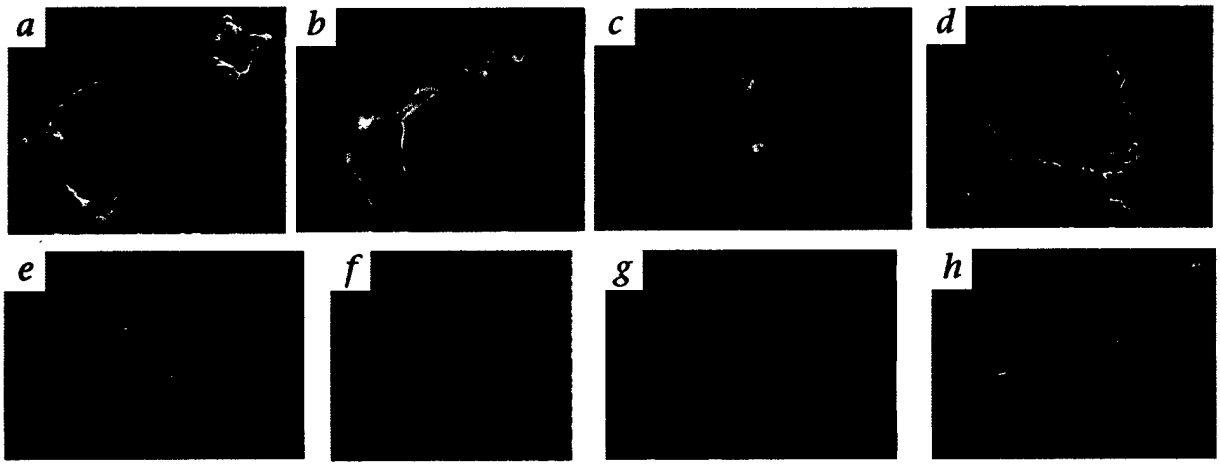

Fig. 3 Colocalization of LyP-1 with lymphatic markers. Fluorescein-conjugated LyP-1 peptide was injected into the tail vein of mice bearing MDA-MB-435 xenografts. *a–e*, LyP-1 (green) colocalizes with red staining for the lymphatic vessel markers LYVE-1 (*a*), podoplanin (*b* and *c*) and VEGFR-3 (*d* and *e*) in reticular and vessel-like structures within the tumor tissue. Some of the peptide fluorescence accumulates in the nuclei of the cells lining the vessels positive for the lymphatic markers and LyP-1, as shown by examination at a higher magnification (podoplanin costaining; *c*) and by using blue counter staining of nuclei with DAPI (*f* and *g*). *h*, LyP-1 fluorescence also partially colocalized with i.v. injected anti-podoplanin antibody in tumor tissue. Magnification, ×200 in *a–d* and *h*; ×400 in *g* and *f*.

target cell would be a transitional cell in between the lymphatic and blood vessel endothelial lineages[6]. There are also some similarities in the distribution of LyP-1 and periodic acid Shiff (PAS)-positive structures in melanomas, which may represent alternate vascular channels[21].

The binding of LyP-1 to putative tumor lymphatics and tumor cells is not universal for all tumors. Although we found LyP-1 to recognize two xenograft tumors and three transgenic mouse tumors, a leukemia (HL-60) and a melanoma (C8161) xenograft were negative. This was the case despite the fact that the C8161 tumors contained lymphatics as identified by positive staining for LYVE-1 and podoplanin and the lack of staining for a blood vessel marker. As the binding of LyP-1 to the cultured tumor cells correlated with its ability to recognize the putative tumor lymphatics in the xenografts, it may be that the tumor cells induce the expression of the LyP-1 binding molecule in the intratumoral lymphatic cells.

Our results suggest that tumor lymphatics may be specialized in a way similar to what has been shown for tumor blood vessels[3,4,22,23]. Moreover, the LyP-1 peptide may make it possible to specifically target tumor lymphatics and their adjacent tumor tissues for destruction. The nuclear localization of fluorescein coupled to LyP-1 suggests that LyP-1 could be a particularly effective carrier of drugs that act inside the nucleus. Given the importance of the lymphatic route in metastasis, such a treatment may destroy the most deadly parts of tumors.

Methods

Mice, cell lines and tumors. MDA-MB-435, KRIB and C8161 cell lines were maintained in DMEM supplemented with 10% FBS. Nude BALB/c mice were subcutaneously injected with $1x10^6$ tumor cells, and tumor-bearing mice were used to prepare cell suspensions and for homing experiments at 3-6 weeks (KRIB or C8161) or 9-12 weeks (MDA-MB-435) post-injection. The animal experimentation was approved by the Burnham Institute Animal Research Committee.

Phage libraries and screening. The libraries were prepared as described[5]. NNK-oligonucleotides encoding a random library of cyclic peptides of the general structure CX_7C (ref. 24) were cloned into the T7Select 415-1 vector according to the manufacturer's instructions (Novagen, Madison, Wisconsin). This vector displays peptides in all 415 copies of the phage capsid protein as a C-terminal fusion.

Tumor-homing phage were isolated from the phage library by combining *ex vivo* and *in vivo* screening. For the *ex vivo* screening, tumor-cell suspensions were prepared from human MDA-MB-435 breast carcinoma xenograft tumors using collagenase (0.5 mg/ml, Sigma) to disperse the tissue. A cell suspension was incubated with the phage library (3.7×10^{10} plaque-forming units (p.f.u.)) overnight at 4 °C and unbound phage were removed by serially washing with 1% BSA in DMEM. Magnetic beads (Dynal, Oslo, Norway) coated with anti-mouse CD31 (MEC 13.3; Pharmingen, San Diego, California) were used to preferentially deplete the tumor-derived cell suspension of blood vessel endothelial cells. Phage bound to the CD31-deficient cell population were rescued and amplified. The phage selection process was repeated 3 times. The *ex vivo* pre-selected phage pool was then subjected to an *in vivo* selection round by injecting it (1.7×10^9 p.f.u.) into the tail vein of a nude mouse bearing an MDA-MB-435 tumor. 48 individual clones were then picked from this *in vivo*-selected, tumor-homing pool and their peptide-encoding inserts were sequenced. Nine peptides appearing more than once were amplified and their ability to bind to cultured cells and tumor-derived cell suspensions was tested[5]. The 5 individual phage that bound better to cell suspensions from MDA-MB-435 tumors than to cultured MDA-MB-435 cells were tested for their ability to home to tumors *in vivo*. In some experiments, the phage were rescued from tissues by treating the tissue with 0.5% NP-40 in PBS.

Peptide synthesis. Peptides were synthesized in our peptide synthesis facility using Fmoc chemistry in a solid-phase synthesizer. The peptides were purified by HPLC, and their sequence and structure was confirmed by mass spectrometry. Fluorescein-conjugated peptides were synthesized as described[25].

Antibodies and immunohistology. To produce antibodies to T7, New Zealand White rabbits were immunized with 10^{10} p.f.u. of T7 nonrecombinant phage (Novagen). The initial immunization was done in complete Freund's adjuvant and boosters were with incomplete Freund's adjuvant. The antibody titer was estimated by using ELISA, and the antiserum was absorbed against BLT5615 bacterial and mouse liver lysates. The LYVE-1 antibody was produced by immunizing New Zealand White rabbits with a peptide encoding the 19 C-terminal residues of mouse LYVE-1 (ref. 10) conjugated to keyhole limpet hemocyanin (KLH; Pierce, Rockford, Illinois). The initial immunization was done in complete Freund's adjuvant and boosters were with incomplete Freund's adjuvant. The antibodies were affinity purified with the peptide coupled to Sulfolink Gel (Pierce) and tested for tissue reactivity by immunofluorescence, where they gave a characteristic lymphatic staining pattern. The specificity of this antibody and that of an antibody against the ectodomain of LYVE-1 (ref. 10) have been reported to be similar[7]. Other primary antibodies used in immunohistochemistry were rat anti-mouse VEGFR-3 (ref. 12) (provided by K. Alitalo and H. Kubo), rat anti-mouse podoplanin[11] (provided by T. Petrova), rat anti-mouse MECA-32 (Pharmingen), rat anti-mouse CD31 (Pharmingen), and biotin anti-mouse H-2Kd, clone SF1-1.1 (Pharmingen).

Tissue distribution of fluorescein-labeled peptides was examined by i.v. injection of the peptide (100 μg in 200 μl PBS) into the tail vein of a mouse. Blood vessels were visualized by i.v. injection of *Lycopersicon esculentum* (tomato) lectin conjugated either to fluorescein or biotin (100 μg in 200 μl of PBS; Vector, Burlingame, California). The biotinyated lectin was detected with streptavidin-conjugated Alexa-594 (red). In some experiments, the anti-podoplanin antibody was similarly injected. The injected materials were allowed to circulate for 5–15 min and the mouse was perfused with 4% paraformaldehyde through the heart. Tissues were removed and frozen in OCT embedding medium (Tissue-Tek, Elkhart, Indiana). The biotin-conjugated lectin was detected with streptavidin-conjugated Alexa-594 (Molecular Probes, Eugene, Oregon) and the anti-podoplanin antibody with goat anti-rat Alexa-488 or Alexa-594 (Molecular Probes).

Note: Supplementary information is available on the Nature Medicine *website.*

Acknowledgments

We thank E. Engvall and E. Pasquale for comments on the manuscript; K. Alitalo, H. Kubo, T. Petrova and M. Quintanilla for antibodies; M. Bernasconi and A. Man for tumor materials; F. Ferrer for peptide synthesis; and R. Newlin for assistance with histology. This study was supported by grants CA74238, CA82715, the Cancer Center Support Grant CA 30199 from the NCI, and grant 99-3339 from the Komen Foundation. P.L. is supported by fellowship 69768 from the Academy of Finland and a fellowship from the Finnish Cultural Foundation. J.A.H. is a recipient of a National Cancer Institute Training Grant fellowship in the Molecular Pathology of Cancer.

Competing interests statement

The authors declare that they have no competing financial interests.

RECEIVED 28 FEBRUARY; ACCEPTED 13 MAY 2002

1. Hanahan, D. & Folkman, J. Patterns and emerging mechanisms of the angiogenic switch during tumorigenesis. *Cell* **86**, 353–364 (1996).
2. Ruoslahti, E. Specialization of tumour vasculature. *Nature Rev. Cancer* **2**, 83–90 (2002).
3. Arap, W., Pasqualini, R. & Ruoslahti, E. Cancer treatment by targeted drug delivery to tumor vasculature in a mouse model. *Science* **279**, 377–380 (1998).
4. Porkka, K., Laakkonen, P., Hoffman, J.A., Bernasconi, M. & Ruoslahti, E. A fragment of the HMGN2 protein homes to the nuclei of tumor cells and tumor endothelial cells *in vivo*. *Proc. Natl. Acad. Sci. USA* (in the press).
5. Hoffman, J.A., Laakkonen, P., Porkka, K., Bernasconi, M. & Ruoslahti, E. *In vivo* and *ex vivo* selections using phage-displayed libraries. in *Phage Display: A Practical Approach* (eds. Clackson, T. & Lowman, H.) (Oxford University Press, Oxford, UK, in the press).

6. Oliver, G. & Detmar, M. The rediscovery of the lymphatic system: old and new insights into the development and biological function of the lymphatic vasculature. *Genes Dev.* **16**, 773–783 (2002).
7. Makinen, T. *et al.* Isolated lymphatic endothelial cells transduce growth, survival and migratory signals via the VEGF-C/D receptor VEGFR-3. *EMBO J.* **20**, 4762–4773 (2001).
8. Chang, Y.S. *et al.* Mosaic blood vessels in tumors: frequency of cancer cells in contact with flowing blood. *Proc. Natl. Acad. Sci.USA* **97**, 14608–14613 (2000).
9. Jackson, D.G., Prevo, R., Clasper, S. & Banerji, S. LYVE-1, the lymphatic system and tumor lymphangiogenesis. *Trends Immunol.* **22**, 317–321 (2001).
10. Prevo, R., Banerji, S., Ferguson, D.J., Clasper, S. & Jackson, D.G. Mouse LYVE-1 is an endocytic receptor for hyaluronan in lymphatic endothelium. *J. Biol. Chem.* **276**, 19420–19430 (2001).
11. Breiteneder-Geleff, S. *et al.* Angiosarcomas express mixed endothelial phenotypes of blood and lymphatic capillaries: Podoplanin as a specific marker for lymphatic endothelium. *Am. J. Pathol.* **154**, 385–394 (1999).
12. Kubo, H. *et al.* Involvement of vascular endothelial growth factor receptor-3 in maintenance of integrity of endothelial cell lining during tumor angiogenesis. *Blood* **96**, 546–553 (2000).
13. Stacker, S.A. *et al.* VEGF-D promotes the metastatic spread of tumor cells via the lymphatics. *Nature Med.* **7**, 186–191 (2001).
14. Skobe, M. *et al.* Induction of tumor lymphangiogenesis by VEGF-C promotes breast cancer metastasis. *Nature Med.* **7**, 192–198 (2001).
15. Beasley, N.J.P. *et al.* Intratumoral lymphangiogenesis and lymph node metastasis in head and neck cancer. *Cancer Res.* **62**, 1315–1320 (2002).
16. Mandriota, S.J. *et al.* Vascular endothelial growth factor-C-mediated lymphangiogenesis promotes tumour metastasis. *EMBO J.* **20**, 672–682 (2001).
17. Leu, A.J., Berk, D.A., Lymboussaki, A., Alitalo, K. & Jain, R.K. Absence of functional lymphatics within a murine sarcoma: a molecular and functional evaluation. *Cancer Res.* **60**, 4324–4327 (2000).
18. Karpanen, T. *et al.* Vascular endothelial growth factor C promotes tumor lymphangiogenesis and intralymphatic tumor growth. *Cancer Res.* **61**, 1786–1790 (2001).
19. Carreira, C.M. *et al.* LYVE-1 is not restricted to the lymph vessels: Expression in normal liver blood sinusoids and down-regulation in human liver cancer and cirrhosis. *Cancer Res.* **61**, 8079–8084 (2001).
20. Valtola, R. *et al.* VEGFR-3 and its ligand VEGF-C are associated with angiogenesis in breast cancer. *Am. J. Pathol.* **154**, 1381–1390 (1999).
21. Maniotis, A.J. *et al.* Vascular channel formation by human melanoma cells *in vivo* and *in vitro*: Vasculogenic mimicry. *Am. J. Pathol.* **155**, 739–752 (1999).
22. Brooks, P.C. *et al.* Integrin αvβ3 antagonists promote tumor regression by inducing apoptosis of angiogenic blood vessels. *Cell* **79**, 1157–1164 (1994).
23. St Croix, B. *et al.* Genes expressed in human tumor endothelium. *Science* **289**, 1197–202 (2000).
24. Smith, G.P. & Scott, J.K. Libraries of peptides and proteins displayed on filamentous phage. *Methods Enzymol.* **217**, 228–257 (1993).
25. Wender, P.A. *et al.* The design, synthesis, and evaluation of molecules that enable or enhance cellular uptake: peptoid molecular transporters. *Proc. Natl. Acad. Sci. USA* **97**, 13003–13008 (2000).

A fragment of the HMGN2 protein homes to the nuclei of tumor cells and tumor endothelial cells *in vivo*

Kimmo Porkka*†, Pirjo Laakkonen*, Jason A. Hoffman*‡, Michele Bernasconi*, and Erkki Ruoslahti*§

*Cancer Research Center, The Burnham Institute, 10901 North Torrey Pines Road, La Jolla, CA 92037; †Helsinki University Central Hospital, Department of Medicine, Division of Hematology, Stem Cell and Basic Science Laboratory, Haartmaninkatu 4, 00029 HUS, Helsinki, Finland; and ‡Program in Molecular Pathology, The Burnham Institute and Department of Pathology, University of California–San Diego School of Medicine, 9500 Gilman Drive, La Jolla, CA 92093

Contributed by Erkki Ruoslahti, March 28, 2002

We used a screening procedure to identify protein domains from phage-displayed cDNA libraries that bind both to bone marrow endothelial progenitor cells and tumor vasculature. Screening phage for binding of progenitor cell-enriched bone marrow cells *in vitro*, and for homing to HL-60 human leukemia cell xenograft tumors *in vivo*, yielded a cDNA fragment that encodes an N-terminal fragment of human high mobility group protein 2 (HMGN2, formerly HMG-17). Upon i.v. injection, phage displaying this HMGN2 fragment homed to HL-60 and MDA-MB-435 tumors. Testing of subfragments localized the full binding activity to a 31-aa peptide (F3) in the HMGN2 sequence. Fluorescein-labeled F3 peptide bound to and was internalized by HL-60 cells and human MDA-MB-435 breast cancer cells, appearing initially in the cytoplasm and then in the nuclei of these cells. Fluorescent F3 accumulated in HL-60 and MDA-MB-435 tumors after an i.v. injection, appearing in the nuclei of tumor endothelial cells and tumor cells. Thus, F3 can carry a payload (phage, fluorescein) to a tumor and into the cell nuclei in the tumor. This peptide may be suitable for targeting cytotoxic drugs and gene therapy vectors into tumors.

angiogenesis | bone marrow cells | progenitor cells | phage libraries | peptides

Tumors induce and sustain the growth of new blood vessels through angiogenesis (1–3). In the initial phases of tumor angiogenesis, new vessels are derived from existing capillaries by sprouting of the endothelial and mural cells (4, 5). Endothelial progenitor cells can be recruited to these new vessels from the bone marrow and from circulation (6–8). The recruitment of these progenitor cells and their proliferation are regulated by angiogenic factors such as vascular endothelial growth factor and angiopoietin-1 (9, 10), but the extent to which they contribute to angiogenesis in normal individuals is unclear. However, they appear to be of major importance in certain situations; Id-mutant mice are defective in angiogenic responses and do not support tumor growth (11), but transplanting wild-type bone marrow into these mice restores the angiogenic responses and allows for tumor growth (12).

The vasculature within tumors expresses distinct molecular markers that are characteristic of angiogenic vessels (13). These markers are also expressed in angiogenic vessels of nonmalignant tissues, such as wounds and inflammatory lesions. They include certain integrins (14, 15), receptors for angiogenic growth factors (16), proteases (17–19), and membrane proteins of unknown functions (20, 21). Pericytes of angiogenic vessels express a membrane proteoglycan known as NG2 or high molecular weight melanoma antigen (22, 23), and the extracellular matrix of angiogenic vessels contains an alternatively spliced form of fibronectin (24).

Several years ago, we developed an approach to study molecular specialization in the vasculature of tumors and normal tissues. The method is based on *in vivo* screening of large libraries of phage-displayed peptides to obtain peptides that have selective tissue affinities and direct the homing of phage to a specific target tissue in mice. When the libraries are injected into the circulation, the method primarily targets tissue-specific differences in endothelial cells. We have previously isolated peptides that home to the vasculature of individual normal tissues and tumors (25, 26).

Our previous tumor-homing peptides bind to molecules characteristic of angiogenic vessels (18, 25). In the present work, we modified the phage procedure to search for markers that would be shared by tumor vasculature and endothelial progenitor cells in the bone marrow. We screened cDNA libraries displayed on phage first on bone marrow cells *ex vivo* and then in tumor-bearing mice *in vivo*. We report a cDNA that encodes a fragment of the nuclear protein high mobility group (HMG) protein 2 (HMGN2). HMGN2 is a highly conserved nucleosomal protein thought to be involved in unfolding higher-order chromatin structure and facilitating the transcriptional activation of mammalian genes (reviewed in ref. 27). We derived a 31-aa synthetic peptide from this HMGN2 fragment, which, when injected i.v., accumulates in the nuclei of tumor endothelial cells and tumor cells. This peptide may find a use as a carrier of therapeutic molecules to the nuclei of tumor cells and tumor endothelial cells. The cell surface receptor for this peptide may be a useful molecular marker of endothelial progenitor cells.

Materials and Methods

Cell Lines and Experimental Animals. Human myeloid leukemia HL-60 (American Type Culture Collection) and MDA-MB-435 human breast carcinoma cell lines were grown in RPMI 1640 media supplemented with 10% FBS (25). To establish xenograft tumors, 2- to 3-month old nude mice (Harlan Sprague–Dawley) were s.c. injected with 10^6 exponentially growing cells in 200 μl of culture media. The animals were used in experiments within 3–5 (HL-60) or 8–10 weeks (MDA-MB-435) of the injection.

Phage Libraries and Screening Protocol. We constructed cDNA libraries by using mRNA purified from normal (human bone marrow, brain, and mouse embryo) and malignant (liver, lung, breast, and colon carcinoma) tissues (CLONTECH) and from mouse spleen and bone marrow (Oligotex Direct mRNA kit, Qiagen, Valencia, CA). The cDNA synthesis with random primers, cloning into the T7Select 10–3b vector, and phage packaging and amplification were done according to the manufacturer's instructions (Novagen). The cDNA libraries were pooled for the phage screening. The screening on isolated primary cells (*ex vivo* selection) and *in vivo* was performed as described (refs. 28 and 29; P.L., K.P., J.A.H., and E.R., unpublished work). In short, 10^9 plaque-forming units (pfu) of the

Abbreviations: HMG, high-mobility group; pfu, plaque-forming units.

§To whom reprint requests should be addressed. E-mail: ruoslahti@burnham.org.

www.pnas.org/cgi/doi/10.1073/pnas.062189599

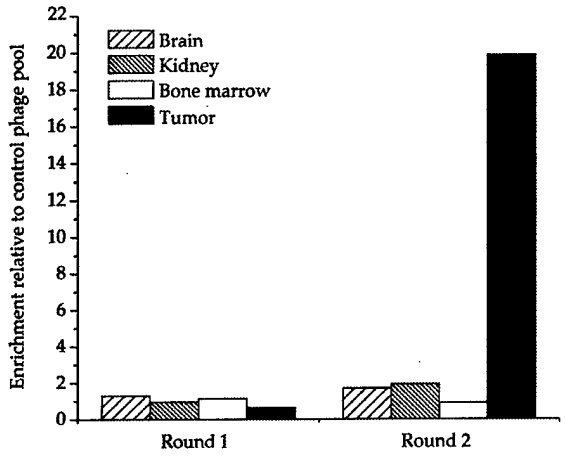

Fig. 1. Phage enrichment *in vivo*. A cDNA phage pool that was preselected for *ex vivo* binding to bone marrow cells was injected into the tail vein of mice. After 10 min of circulation, the mice were perfused through the heart, and phage was rescued from various organs, amplified, and used for subsequent rounds of selection. Fold enrichment of selected phage pool relative to the unselected cDNA phage library pool is shown.

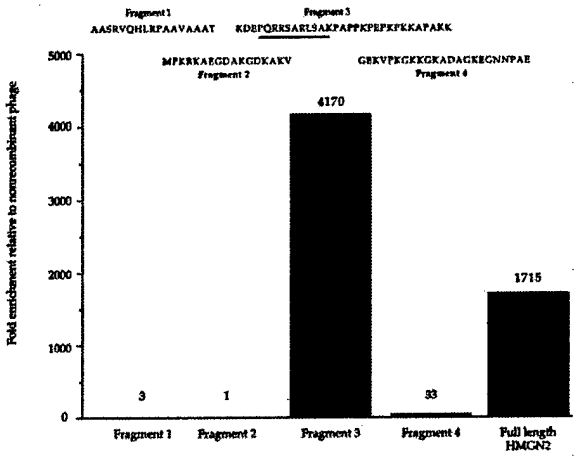

Fig. 2. Localization of the HMGN2-N cell binding site. The sequence and cell binding activity of individual HMGN2-N fragments. Inserts encoding for the various fragments were cloned into T7 phage, and the phage preparations were tested for binding to primary cells from HL-60 xenograft tumors. After a 1-h incubation at 4°C, the cells were washed and phage-quantified (the pfu are indicated above the columns). The enrichment is shown relative to a control phage (nonrecombinant T7 phage). One experiment representative of four is shown. The sequence encoded by exon 3 of HMGN2 is underlined.

phage library were incubated on target cells overnight at 4°C. Unbound phage were removed by extensive washing, and the phage bound to cells were rescued, amplified, and used for the subsequent round of selection. After two rounds of *ex vivo* selection, the phage pool was subjected to *in vivo* selection by injecting the pool (10^9 pfu) into the tail vein of a nude mouse bearing a HL-60 xenograft tumor. After two rounds of *in vivo* selection, 96 clones were selected from this tumor-homing pool and their protein-encoding inserts were sequenced.

Isolation of Murine Bone Marrow Progenitor Cells. Mouse bone marrow was obtained by flushing both femoral and tibial bones with 3 ml of cold media (DMEM supplemented with 10% FBS). The bone marrow was then depleted of cells expressing common lineage-specific markers by using antibodies coupled to paramagnetic beads (StemSep Murine Kit, StemCell Technologies, Vancouver). The antibodies used were against mouse CD5 (clone Ly-1), myeloid differentiation antigen (Gr-1), CD45R (B220), erythroid cells (TER119), CD11b (Mac-1), and neutrophils (7–4) (StemCell Technologies). The remaining megakaryocytes were removed by filtering through a 30-μm nylon mesh filter (Miltenyi Biotec, Auburn, CA).

Flow Cytometry. Human bone marrow specimens analyzed in this study represented excess material from samples collected for diagnostic purposes from adults with hematological malignancies. Informed consent was obtained before sample collection. A total of 2 ml of bone marrow was aspirated from the posterior iliac crest and stored in a citrate anticoagulant. Mononuclear cells were isolated by gradient centrifugation (Ficoll-Paque PLUS, Amersham Pharmacia) and incubated in RPMI 1640 media supplemented with 10% FBS for 2 h at 37°C. The cells were then transferred to 4°C and incubated with 1–2 μM fluorescein-conjugated peptides for 45 min and subsequently stained with PerCP- or phycoerythrin-conjugated CD34 and CD45 antibodies (Becton Dickinson) for 30 min. The sample was analyzed with either a FACSCalibur or a LSR flow cytometer (Becton Dickinson), and 100,000 events were collected.

Anti-T7 Antibodies. New Zealand White rabbits were immunized with 10^{10} pfu of T7 nonrecombinant phage. The initial immunization was done in complete Freund's adjuvant and boosters were in incomplete Freund's adjuvant. The antiserum was absorbed on BLT5615 bacterial and mouse liver lysates, and the antibody titer was estimated by ELISA.

Peptides. Peptides were synthesized with an automated peptide synthesizer by using standard solid-phase fluorenylmethoxycarbonyl chemistry (30). During synthesis, the peptides were labeled with fluorescein with an amino-hexanoic acid spacer as described (31). The concentration of unlabeled peptides was determined by weighing and from absorbance at 230 nm (32).

Histology. Tissue distribution of homing ligands was examined by i.v. injection of fluorescein-coupled peptides (100 μl of a 1 mM solution) into the tail vein of anesthesized mice bearing xenografts. Blood vessels were visualized by i.v. injecting 200 μl of 0.5 μg/μl biotin-conjugated tomato lectin (Vector Laboratories). The injected materials (first peptide, then lectin) were allowed to circulate for 15 min, and the mouse, which remained anesthesized throughout the experiment, was perfused through the heart with 4% paraformaldehyde. Organs were removed and frozen in OCT embedding medium (Tissue-Tek, Elkhart, IN). The biotin-conjugated lectin was detected with streptavidin-Alexa 594 (Molecular Probes), mounted with Vectashield- 4′,6-diamidino-2-phenylindole (Vector Laboratories), and examined under an inverted fluorescent microscope.

Results

Tumor-Homing HMGN2 Fragment. Hematopoietic and endothelial precursors have a common cell of origin (hemangioblast) and share several phenotypic characteristics. We devised a phage screening procedure that would capitalize on this shared phenotype and select clones that bind to both primitive bone marrow cells and angiogenic endothelial cells. The screening procedure included a preselection on lineage-depleted mouse bone marrow cells (putative progenitor cells) *ex vivo* and further selection for homing to HL-60 xenograft tumors *in vivo*.

After two rounds of preselection on lineage-depleted mouse

CELL BIOLOGY

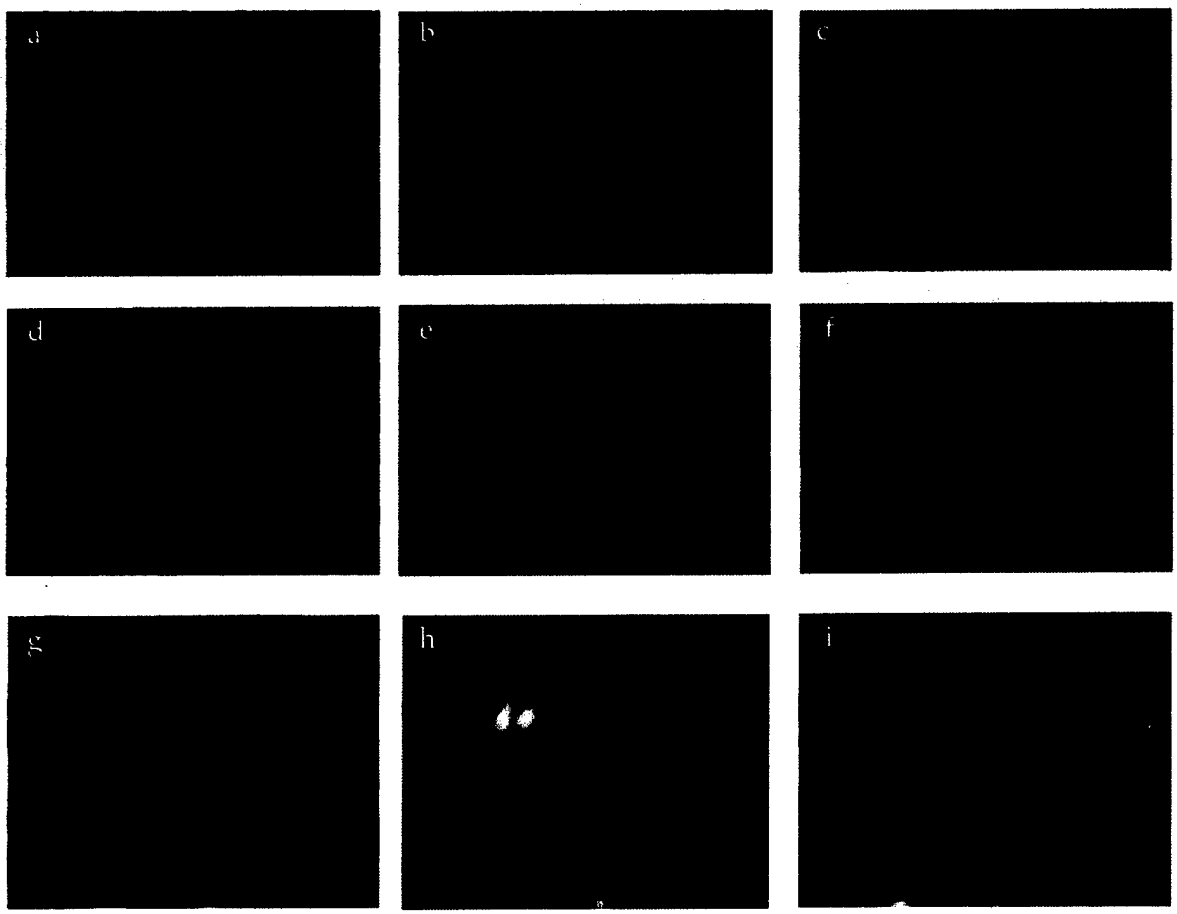

Fig. 3. Tissue localization of i.v.-injected F3 peptide. HMGN2-N F3 peptide and ARALPSQRSR control peptide were conjugated to fluorescein. Each labeled peptide was injected into the tail vein of mice bearing HL-60 or MDA-MB-435 xenografts. The peptide injection was followed 10 min later by an injection of biotinylated tomato lectin. After another 5 min, the mice were perfused through the heart with a fixative solution, and the organs were dissected, sectioned, and stained with streptavidin-Alexa 594. The slides were counterstained with 4′,6-diamidino-2-phenylindole and examined under an inverted fluorescent microscope. (*e*) An HL-60 tumor section from a mouse injected with fluorescein-labeled ARALPSQRSR control peptide, all other panels are from mice injected with fluorescein-labeled F3. (*a*) HL-60 tumor; (*b*) brain; (*c*) skin; (*d*) gut; (*e*) ARALPSQRSR control peptide in HL-60 tumor; (*f*) fluorescein-labeled F3 in an MDA-MB-435 tumor; (*g*) a higher magnification view from *a* showing the localization of F3 (green), lectin-stained vasculature (red), and 4′,6-diamidino-2-phenylindole-stained nuclei (blue). The green and blue images are shown individually in *h* and *i*. (Magnifications: *a*, *b*, and *e*, ×200; *c* and *d*, ×100; and *f–i*, ×400.)

bone marrow cells, the resulting phage pool was injected in nude mice bearing HL-60 tumors. The selected phage pool showed a 20-fold enrichment for tumor homing relative to the unselected library after two rounds of *in vivo* selection (Fig. 1). Sequencing showed that the predominant cDNA in this pool was a 270-bp clone that contained an ORF encoding the first 73 N-terminal amino acids of the human HMGN2 protein; the clone also contained 51 bp from the 5′ noncoding sequence. We designated this clone HMGN2-N. Additional HMGN2 clones were also isolated from the phage pool; they all shared a common sequence corresponding to exons 3 and 4 in the HMGN2 sequence. The same HMGN2-N cDNA clone was also isolated in another independent screening.

The HMGN2-N phage homed to the HL-60 tumors to about the same extent as the selected pool (data not shown). The injected phage also accumulated in the kidneys, but only when the number of phage injected was small, 10^9 pfu). Tumor homing was obtained both at this input level, and when 10^{12} pfu of phage were injected. We do not know the reason for the dose effect. About 1,000 times more HMGN2-N phage than nonrecombinant T7 phage bound to cultured HL-60 and MDA-MB-435 cells. Cell suspensions made from HL-60 tumors also bound the HMGN2-N phage with a 1,000-fold greater specificity relative to the control phage. Phage clones encoding fragments of some other proteins were identified in the screenings, but these fragments homed less well to tumors than HMGN2-N and were not studied further.

HMGN2-N Binding Domain and Specificity. To identify the HMGN2-N domain responsible for the cell binding and *in vivo* homing, we constructed phage that display a set of fragments from HMGN2-N. The fragments were designed to include the complete exon sequences of the HMGN2 gene. A 31-aa fragment encoded by exons 3 and 4 (F3 peptide) showed substantial tumor cell binding (Fig. 2); F3 corresponds to the nucleosomal binding domain of HMGN2. The binding of the F3-displaying phage to tumor cells was inhibited by free F3 peptide in a dose-dependent fashion; complete inhibition was achieved with

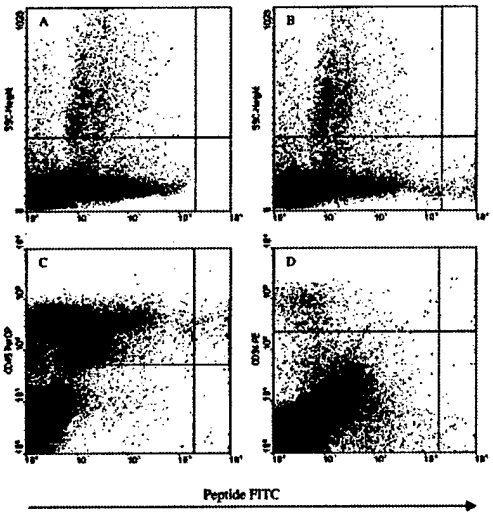

Fig. 4. FACS profile of bone marrow cells labeled with fluorescent F3 peptide and antibodies against cell differentiation markers. Fluorescein-labeled peptides, F3 and ARALPSQRSR control peptide at 2 μM, were incubated with gradient-depleted bone marrow cells and analyzed in a flow cytometer. (*A*) Control peptide (number/percentage of cells in lower right quadrant: 1/0.0); (*B*) F3 peptide (308/0.88); (*C*) F3 vs. CD45 (77% CD45-positive); (*D*) F3 vs. CD34 (75% CD34-negative).

100 μM peptide. The background binding of nonrecombinant phage was unaffected by this peptide. We further divided the F3 peptide into two peptides. Phage displaying exon 3, PQRRSARLSA, also bound to tumor cells but less well than F3. The specificity of the cell binding was further confirmed by comparing HL-60 cell binding of HMGN2 exon 3-displaying phage (insert sequence, PQRRSARLSA) and the homologous HMGN1 exon 3-displaying phage (insert sequence, PKRRSARLSA). The HMGN1 phage bound 90% less than the HMGN2 phage, indicating that the single amino acid change from glutamine to lysine substantially changes the cell binding specificity of the fragment. Database searches showed that the PQRRSARLSA sequence is present in a number of expressed sequence tags, the sequence of which is otherwise different from that of HMGN2. Thus, proteins other than HMGN2 may possess the same cell binding activity.

Tissue and Cellular Localization of F3 Peptide. To be able to study the localization of the F3 peptide in tissues and cells, we synthesized this peptide as a conjugate with fluorescein. The labeled peptide was injected i.v. into mice bearing HL-60 or MDA-MB-435 tumors, and the localization of fluorescence was studied in tissues collected 10–15 min later. Strong fluorescence was seen in the tumor tissue (Fig. 3*a*), whereas little or no specific fluorescence was detected in the brain, liver, and spleen; the result for the brain is shown in Fig. 3*b*. F3 was present in a small population of cells in the skin and gut (Fig. 3 *c* and *d*). Diffuse fluorescence accumulated in proximal tubules of kidneys. Fluorescein-labeled scrambled exon 3 peptide (ARALPSQRSR)

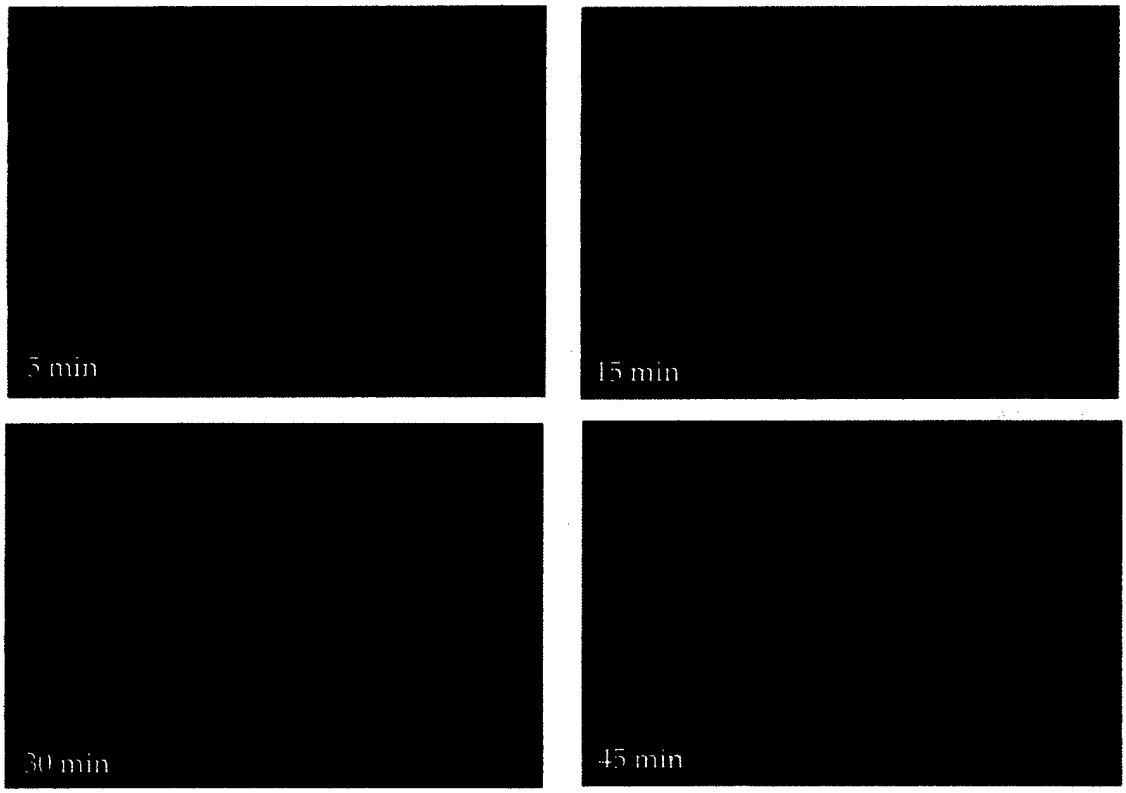

Fig. 5. Kinetics of uptake and nuclear translocation of F3 peptide in cultured MDA-MB-435 cells. The cells were incubated with fluorescein-labeled F3 (1 μM) for the indicated length of time at 37°C, washed, fixed, and examined under an inverted fluorescent microscope.

CELL BIOLOGY

produced a similar fluorescence pattern in the kidney, but was essentially undetectable in other tissues, including the HL-60 tumors (Fig. 3*e*). Thus, the fluorescence in the kidneys is presumably caused by nonspecific uptake of peptides, or fluorescein, from the glomerular filtrate.

In the HL-60 leukemia tumor tissue, F3 localized in tumor cells and cells lining tumor blood vessels, presumably the endothelial cells. The fluorescence was predominantly located in the nuclei (Fig. 3 *a* and *g–i*). Most of the tumor cells containing fluorescence were around blood vessels. In MDA-MB-435 breast cancer tumors, F3 also accumulated in the endothelial cells and tumor cells. In some microscopic fields, the F3 fluorescence was essentially limited to the endothelial cells, providing a particularly clear view of F3 within endothelial cells and their nuclei (Fig. 3*f*). Similar tumor localization was obtained with F3 coupled to another fluorescent molecule, rhodamine (not shown).

F3 also specifically bound to a small (0.3–0.8% of mononuclear cells) cell population in human bone marrow (Fig. 4). The F3-positive cells were lymphocyte-sized, agranular, CD45-positive, and mostly CD34-negative. This marker profile is similar to that of the lineage-depleted mouse bone marrow cell population we used in the phage preselection.

Cellular uptake and nuclear translocation of the F3 peptide were also observed in cultured HL-60 cells and MDA-MB-435 cells *in vitro*. The fluorescein-labeled peptide appeared in the cytoplasm of the cells where it was diffusely distributed (Fig. 5). Nuclear fluorescence started appearing at 30 min, and after 1 h most of the fluorescence was in the nuclei. The internalization process appeared to be slower *in vitro* than *in vivo*, possibly because of a more avid binding of the peptide to the target cells *in vivo*. The cellular uptake did not depend on the nature of the fluorescent dye, as rhodamine-labeled F3 also accumulated in the nuclei of the MDA-MB-435 cells (not shown). The D-amino acid form of F3 was also internalized by the MDA-MB-435 cells, but more slowly than the L-form, and it did not accumulate in the nucleus (Fig. 6). The uptake was energy dependent, as it was slower at 4°C than at 37°C (not shown).

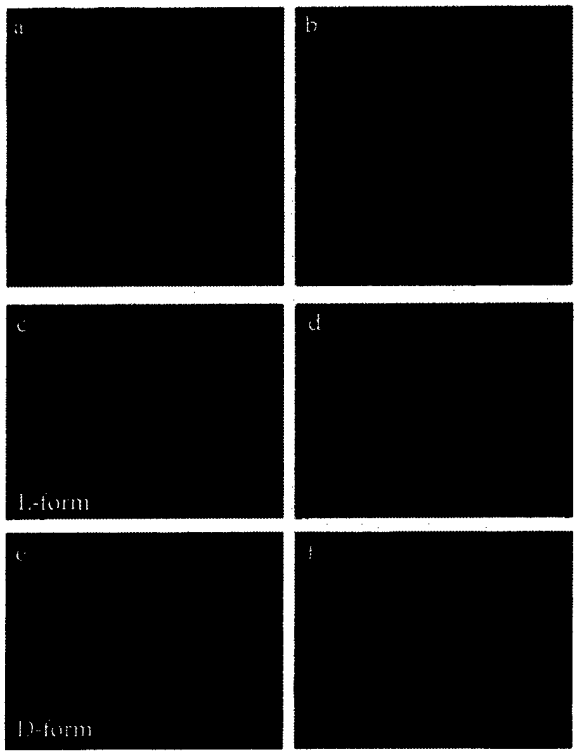

Fig. 6. Nuclear localization of the L- and D-forms of the F3 peptide. Nuclear localization in HL-60 cells of F3 (*a*) or ARALPSQRSR control peptide (*b*). (*c–f*) Uptake by MDA-MB-435 cells of F3 synthesized either from L or D amino acids. The cells were treated as in Fig. 5A and stained with 4′,6-diamidino-2-phenylindole before examination under a confocal (*a* and *b*) or inverted fluorescent microscope (*c–f*). (*c* and *e*) Peptide staining (green); (*d* and *f*) nuclear staining (blue). (Magnifications: *a and b*, ×400; *c–f*, ×200.)

Discussion

We describe a tumor-homing protein fragment and a peptide derived from it, both of which bind to tumor blood vessels and tumor cells. The peptide homes selectively into tumors and has the remarkable property of being able to carry a payload into the nuclei of the target cells.

In this work, we used phage-displayed cDNA libraries *in vivo* to search for phage capable of homing to tumors, especially to their vasculature. Our thinking was that any proteins or protein fragments identified from the cDNA libraries might have higher affinities for tumor vasculature than the relatively short peptides obtained from random peptide libraries in previous work (13). Another expectation was that we might identify proteins that are functionally linked to the growth of tumors or their blood vessels. The cDNA library screening revealed a remarkably potent homing peptide, F3, indicating that the first expectation may have been fulfilled. Whether HMGN2, the nuclear protein that F3 is derived from, might have an extracellular function remains to be seen. It is interesting to note that there are some similarities between HMGN2 and amphoterin (HMGB1, formerly HMG-1), an intracellular and nuclear protein that is secreted in a signal sequence-independent manner and regulates cell migration and invasion through binding to its cell surface receptor, RAGE (33, 34). Blockade of RAGE-amphoterin signaling decreased tumor growth and metastases in mice (35).

Another modification to the original *in vivo* phage screening protocol was to enrich the library by selecting on isolated bone marrow cells before the *in vivo* screening step for tumor homing. Our aim was to identify proteins or peptides that would recognize an epitope shared by bone marrow progenitor cells and tumor endothelial cells. The F3 peptide appears to fulfill this expectation. It recognizes a minor population of progenitor cell-like bone marrow cells, the closer identity of which remains to the established, and it also binds to endothelial cells in tumors. This "dual target" screening approach is likely to further expand the utility of *in vivo* phage screening.

The specificity of the F3 peptide is broader than binding of the bone marrow subpopulation and tumor endothelial cells; F3 binding is a shared property of tumor cells and tumor endothelial cells. F3 appears to recognize a variety of tumor types; all tumors we have tested, including the TRAMP mouse prostate carcinomas (36), have been positive for F3 binding. In addition to the tumors and bone marrow, systemically injected F3 recognizes a minor population in both the normal skin and the gut. These cells are not associated with the vasculature, but their tissue localization did not suggest any obvious identity for these cells. The F3 binding specificity in the bone marrow and in tumors suggests that the positive cells in the skin and gut may represent some kind of a progenitor cell.

The strong accumulation of fluorescein-labeled F3 in tumor vasculature and tumor cells suggests that this peptide may be useful in targeting therapeutic agents into tumors. Other homing peptides isolated by *in vivo* phage display have given promising results in this regard (25, 37, 38). As fluorescein and rhodamine conjugated to F3 accumulate in tumor tissue, one can expect a drug conjugate to do the same.

A feature of F3 that makes it uniquely promising for drug targeting applications is its uptake by cells and its ability to carry a payload into the cell nucleus. We saw intracellular accumulation of fluorescence from fluorescein-labeled F3 in the cytoplasm of the target cells both *in vitro* and *in vivo*. The fluorescence accumulation was particularly striking in the nucleus. The F3 peptide is highly basic and is apparently recognized by the nuclear import machinery. The D-form of F3 also enters the cells, although it is not efficiently translocated into the nucleus. These properties are reminiscent of the cellular uptake and nuclear translocation of highly basic peptides from Tat protein and certain homeobox proteins (39–41). Such peptides are commonly used to introduce proteins and genes into cells. The mechanisms whereby these peptides enter cells are poorly understood, but their internalization is known not to require cellular energy. We find that the internalization of fluorescein-labeled F3 by tumor cells does not take place at 4°C, indicating energy dependence. A more important difference is that F3 only enters certain types of cells, whereas no cell type preference has been reported for other internalizing peptides. The cell type specificity of F3 can offer unique advantages. The numerous anticancer drugs that act in the nucleus (42) could particularly benefit from the nuclear-targeting capability provided by the F3 peptide.

We thank Dr. Edward Monosov for microscopy, Dr. Satu Mustjoki for help with flow cytometry, Dr. Fernando Ferrer for peptide synthesis, and Dr. Eva Engvall for comments on the manuscript. This study was supported by Grants CA74238, CA82713, and CA 30199 (Cancer Center Support Grant) from the National Cancer Institute and Grant 99-3339 from the Komen Foundation. K.P. is supported by the Finnish Medical Foundation, P.L. by fellowships from the Academy of Finland and the Finnish Cultural Foundation, J.A.H. by a National Cancer Institute Training Grant, and M.B. by a Swiss National Science Foundation Fellowship.

1. Hanahan, D. & Folkman, J. (1996) *Cell* **86,** 353–364.
2. Jain, R. K. (1997) *Adv. Drug Delivery Rev.* **26,** 71–90.
3. Hanahan, D. & Weinberg, R. A. (2000) *Cell* **100,** 57–70.
4. Holash, J., Maisonpierre, P. C., Compton, D., Boland, P., Alexander, C. R., Zagzag, D., Yancopoulos, G. D. & Wiegand, S. J. (1999) *Science* **284,** 1994–1998.
5. Yancopoulos, G. D., Davis, S., Gale, N. W., Rudge, J. S., Wiegand, S. J. & Holash, J. (2000) *Nature (London)* **407,** 242–248.
6. Davidoff, A. M., Ng, C. Y., Brown, P., Leary, M. A., Spurbeck, W. W., Zhou, J., Horwitz, E., Vanin, E. F. & Nienhuis, A. W. (2001) *Clin. Cancer Res.* **7,** 2870–2879.
7. Asahara, T., Murohara, T., Sullivan, A., Silver, M., van der Zee, R., Li, T., Witzenbichler, B., Schatteman, G. & Isner, J. M. (1997) *Science* **275,** 964–967.
8. Shi, Q., Rafii, S., Wu, M. H., Wijelath, E. S., Yu, C., Ishida, A., Fujita, Y., Kothari, S., Mohle, R., Sauvage, L. R., *et al.* (1998) *Blood* **92,** 362–367.
9. Hattori, K., Dias, S., Heissig, B., Hackett, N. R., Lyden, D., Tateno, M., Hicklin, D. J., Zhu, Z., Witte, L., Crystal, R. G., *et al.* (2001) *J. Exp. Med.* **193,** 1005–1014.
10. Asahara, T., Takahashi, T., Masuda, H., Kalka, C., Chen, D., Iwaguro, H., Inai, Y., Silver, M. & Isner, J. M. (1999) *EMBO J.* **18,** 3964–3972.
11. Lyden, D., Young, A. Z., Zagzag, D., Yan, W., Gerald, W., O'Reilly, R., Bader, B. L., Hynes, R. O., Zhuang, Y., Manova, K. *et al.* (1999) *Nature (London)* **401,** 670–677.
12. Lyden, D., Hattori, K., Dias, S., Costa, C., Blaikie, P., Butros, L., Chadburn, A., Heissig, B., Marks, W., Witte, L., *et al.* (2001) *Nat. Med.* **7,** 1194–1201.
13. Ruoslahti, E. (2000) *Semin. Cancer Biol.* **10,** 435–442.
14. Kim, S., Bell, K., Mousa, S. A. & Varner, J. A. (2000) *Am. J. Pathol.* **156,** 1345–1362.
15. Brooks, P. C., Montgomery, A. M., Rosenfeld, M., Reisfeld, R. A., Hu, T., Klier, G. & Cheresh, D. A. (1994) *Cell* **79,** 1157–1164.
16. Korpelainen, E. I. & Alitalo, K. (1998) *Curr. Opin. Cell Biol.* **10,** 159–164.
17. Bergers, G., Brekken, R., McMahon, G., Vu, T. H., Itoh, T., Tamaki, K., Tanzawa, K., Thorpe, P., Itohara, S., Werb, Z. & Hanahan, D. (2000) *Nat. Cell Biol.* **2,** 737–744.
18. Pasqualini, R., Koivunen, E., Kain, R., Lahdenranta, J., Sakamoto, M., Stryhn, A., Ashmun, R. A., Shapiro, L. H., Arap, W. & Ruoslahti, E. (2000) *Cancer Res.* **60,** 722–727.
19. Silletti, S., Kessler, T., Goldberg, J., Boger, D. L. & Cheresh, D. A. (2001) *Proc. Natl. Acad. Sci. USA* **98,** 119–124.
20. St Croix, B., Rago, C., Velculescu, V., Traverso, G., Romans, K. E., Montgomery, E., Lal, A., Riggins, G. J., Lengauer, C., Vogelstein, B. & Kinzler, K. W. (2000) *Science* **289,** 1197–1202.
21. Carson-Walter, E. B., Watkins, D. N., Nanda, A., Vogelstein, B., Kinzler, K. W. & St Croix, B. (2001) *Cancer Res.* **61,** 6649–6655.
22. Schlingemann, R. O., Rietveld, F. J., de Waal, R. M., Ferrone, S. & Ruiter, D. J. (1990) *Am. J. Pathol.* **136,** 1393–1405.
23. Ozerdem, U., Grako, K. A., Dahlin-Huppe, K., Monosov, E. & Stallcup, W. B. (2001) *Dev. Dyn.* **222,** 218–227.
24. Nilsson, F., Kosmehl, H., Zardi, L. & Neri, D. (2001) *Cancer Res.* **61,** 711–716.
25. Arap, W., Pasqualini, R. & Ruoslahti, E. (1998) *Science* **279,** 377–380.
26. Ruoslahti, E. & Rajotte, D. (2000) *Annu. Rev. Immunol.* **18,** 813–827.
27. Bustin, M. (1999) *Mol. Cell. Biol.* **19,** 5237–5246.
28. Rajotte, D., Arap, W., Hagedorn, M., Koivunen, E., Pasqualini, R. & Ruoslahti, E. (1998) *J. Clin. Invest.* **102,** 430–437.
29. Hoffman, J., Laakkonen, P., Porkka, K., Bernasconi, M. & Ruoslahti, E. (2002) in *Phage Display: A Practical Approach*, eds. Clarkson, T. & Lowman, H. (Oxford Univ. Press, Oxford), in press. .
30. Atherton, E. & Sheppard, R. (1989) *Solid-Phase Peptide Synthesis* (IRL, Oxford).
31. Wender, P. A., Mitchell, D. J., Pattabiraman, K., Pelkey, E. T., Steinman, L. & Rothbard, J. B. (2000) *Proc. Natl. Acad. Sci. USA* **97,** 13003–13008.
32. Ehresmann, B., Imbault, P. & Weil, J. H. (1973) *Anal. Biochem.* **54,** 454–463.
33. Hori, O., Brett, J., Slattery, T., Cao, R., Zhang, J., Chen, J. X., Nagashima, M., Lundh, E. R., Vijay, S., Nitecki, D., *et al.* (1995) *J. Biol. Chem.* **270,** 25752–25761.
34. Fages, C., Nolo, R., Huttunen, H. J., Eskelinen, E. & Rauvala, H. (2000) *J. Cell Sci.* **113,** 611–620.
35. Taguchi, A., Blood, D. C., del Toro, G., Canet, A., Lee, D. C., Qu, W., Tanji, N., Lu, Y., Lalla, E., Fu, C., *et al.* (2000) *Nature (London)* **405,** 354–360.
36. Gingrich, J. R., Barrios, R. J., Morton, R. A., Boyce, B. F., DeMayo, F. J., Finegold, M. J., Angelopoulou, R., Rosen, J. M. & Greenberg, N. M. (1996) *Cancer Res.* **56,** 4096–4102.
37. Arap, W., Haedicke, W., Bernasconi, M., Kain, R., Rajotte, D., Krajewski, S., Ellerby, M. H., Bredesen, D. E., Pasqualini, R. & Ruoslahti, E. (2002) *Proc. Nat. Acad. Sci. USA* **99,** 1527–1531.
38. Curnis, F., Sacchi, A., Borgna, L., Magni, F., Gasparri, A. & Corti, A. (2000) *Nat. Biotechnol.* **18,** 1185–1190.
39. Lindgren, M., Hallbrink, M., Prochiantz, A. & Langel, U. (2000) *Trends Pharmacol. Sci.* **21,** 99–103.
40. Schwarze, S. R., Ho, A., Vocero-Akbani, A. & Dowdy, S. F. (1999) *Science* **285,** 1569–1572.
41. Gallouzi, I. E. & Steitz, J. A. (2001) *Science* **294,** 1895–1901.
42. Hurley, L. H. (2002) *Nat. Rev. Cancer* **2,** 188–200.